arXiv:1510.05171v2 [physics.bio-ph] 11 Nov 2015

Interplay of curvature-induced micro- and nanodomain structures in multicomponent lipid bilayers

Leonie Brodbek · Friederike Schmid

Received: date / Accepted: date

Abstract We discuss different mechanisms for curvature-induced domain formation in multicomponent lipid membranes and present a theoretical model that allows us to study the interplay between the domains. The model represents the membrane by two coupled monolayers, which each carry an additional order parameter field describing the local lipid composition. The spontaneous curvature of each monolayer is coupled to the local composition; moreover, the lipid compositions on opposing monolayers are coupled to each other. Using this model, we calculate the phase behavior of the bilayer in mean-field approximation. The resulting phase diagrams are surprisingly complex and reveal a variety of phases and phase transitions, including a decorated microdomain phase where nanodomains are aligned along the microdomain boundaries. Our results suggest that external membrane tension can be used to control the lateral organization of nanodomains (which might be associated with lipid "rafts") in a multicomponent lipid bilayer.

Keywords Lipid bilayers · Multicomponent membranes · Lipid Rafts · Ginzburg-Landau theory · Elasticity · Curvature

1 Introduction

Biomembranes are not homogeneous [1]. They consist of a self-assembled lipid bilayer which acts as a support for proteins and other biomolecules [2]. In the last decades, there is increasing evidence that biomembranes are laterally structured [1], and this structure is believed to be important for their biological function. For example, the so-called lipid raft hypothesis states that biomembranes are often filled with nanodomains, which typically have sizes between 10 to 100 nm, a higher cholesterol content and higher local order [3,4,5,6,7,8,9]. Indirect evidence for the existence of such rafts is provided, *e.g.*, by superresolution images showing nanoscopic clusters of raft-associated proteins in membranes [10,11,12]. However, the main forces driving this internal organization of membranes have not yet been identified unambiguously. In particular, the role of the lipids and the question whether and how they contribute to the structuring of membranes is still discussed controversially.

On the one hand, it is argued that the formation of nanoscopic or larger protein clusters in membranes could be driven by the proteins alone. On the other hand, nano- and microstructures have also been observed in pure lipid membranes. Already one-component phospholipid membranes exhibit a modulated "ripple phase" in the transition region between the high temperature fluid phase and the low-temperature gel phase [13,14,15,16,17,18]. Experimental evidence for nanodomains with properties similar to those attributed to rafts has been provided by atomic force microscopy [19] and neutron scattering [20,21,22,23]. On larger scales, multicomponent giant vesicles were found to feature ordered patterns of micron-size domains under certain circumstances [24]. Lateral phase separation was observed in model multicomponent vesicles [25,26,27] and in plasma vesicles extracted from living rat cells [28], and large up to micron-size critical clusters could be visualized in the vicinity of critical points [19,28,29,30,31].

L. Brodbek
Institut für Physik, Johannes Gutenberg-Universität Mainz, DE

F. Schmid
Institut für Physik, Johannes Gutenberg-Universität Mainz, DE E-mail: friederike.schmid@uni-mainz.de

Several physical mechanism have been proposed that may generate micro- or nanostructures in pure lipid membranes [32]: One, mentioned above, is critical cluster formation in the vicinity of a demixing phase transition [19,29,31]. A second suggestion is that line-active molecules in multicomponent mixtures may reduce the line tension and eventually turn an originally phase-separated mixture into a microemulsion [33,34,35,36, 37,38,39,40]. In the present paper, we focus on a third generic class of domain-stabilizing mechanism in membranes: The formation of microemulsions or modulated structures due to curvature-induced elastic interactions.

Two variants of such a mechanism have been proposed in the literature. In the first (termed I hereafter), it is assumed that the two opposing leaflets tend to have different lipid composition, and that this imposes a spontaneous curvature on the *bilayer* as a whole [41]. A tensionless membrane responds by bending around [42]. If tension is applied, it is forced to be planar, and this creates elastic stress. The membrane reacts by forming staggered domains with curvatures of opposite sign. This effect is illustrated in Fig. 1a). It was first proposed by Andelman and coworkers and further investigated by a number of authors [41,42,43,44,45,46, 47,48]. Schick and coworkers argued that it might account for raft formation in membranes [45,46,47]. The characteristic length scales of the domains are in the range of 100 *nm* to micrometers and diverge for tensionless membranes.

The second mechanism (termed II) was recently proposed in our group [18,49]. It assumes that the lipids tend to demix laterally, but the lipid composition on opposing leaflets are preferably in registry. Different lipid compositions are associated with different spontaneous curvature parameters in the *monolayer*. Since the membrane as a whole remains planar, this also creates elastic stress, which is relieved by keeping domain sizes finite. The effect is illustrated in Fig. 1b). Characteristic length scales according to this mechanism are in the range of 10 nm and depend on the membrane material. We have argued that the same effect could also account for the formation of modulated ripple states, which also have characteristic wave lengths in the same order of magnitude, hence ripples and nanodomains in lipid bilayers could be closely related phenomena.

Both mechanisms have in common that they are driven by a coupling between lipid composition and spontaneous curvature. The main difference lies in the nature of the local correlation between the lipid compositions on the two leaflets. Mechanism I assumes that domains are anticorrelated, which favors microdomains. Mechanism II assumes that domains are in registry, which favors nanodomains. Experimentally, it has been

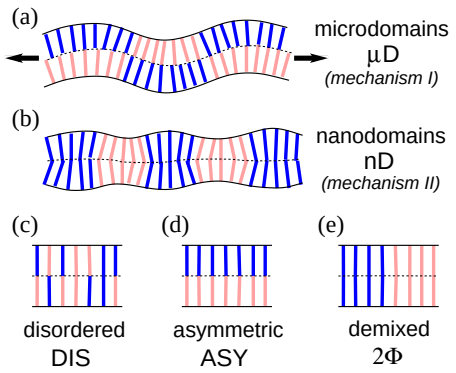

Fig. 1 Curvature-induced domains in mixed bilayers: (a) microdomains formed by mechanism I [41,43,45] (b) nanodomains formed by mechanism II [18,49]. Panels (c-e) show homogeneous membrane states that are also considered in this paper: (c) symmetric disordered state, (d) asymmetric state (e) lateral phase separation

reported that domains on opposing leaflets tend to be in registry [50]. However, the correlation is never perfect, and we shall see below that microdomains may be energetically favorable under certain circumstances even in systems where the coupling between lipid compositions on opposing leaflets is weakly positive.

The purpose of the present paper is to provide a unified picture of curvature-induced phenomena in mixed lipid bilayers. We propose an elastic theory which reproduces both the mechanisms I and II of domain formation. Using mean-field approximation, we can assess the influence of membrane tension, curvature coupling, and composition coupling across leaflets on the bilayer structure, and calculate a representative set of phase diagrams which demonstrate the complex interplay between microdomain and nanodomain formation in these systems.

Our paper is organized as follows. In the next section, we introduce the framework of our theoretical approach and derive a Ginzburg-Landau model which describes both nanodomain and microdomain formation. In Section 3 we present and analyze the possible phase diagrams of this system, which we have calculated analytically within mean-field approximation and a variational single-mode Ansatz. The results are summarized and discussed in Section 4.

2 Theoretical framework

Our theory is based on an elastic model for membranes that describes the lipid bilayer by a system of two coupled elastic monolayers [51,52,53,54]. Each monolayer is represented by a two-dimensional manifold that describes the position of the monolayer-water interface in

a coarse-grained sense. We assume that the membrane is planar on average and aligned in the (x, y) plane, and that bubbles and overhangs can be neglected. Each monolayer surface can then be parametrized by a function $z_i(x, y)$ (where $i = 1, 2$ and $z_1 < z_2$). We consider a symmetric situation where both monolayers have the same elastic properties, except that their spontaneous curvatures c_i may vary locally and differ from each other. We adopt a sign convention according to which c_i is positive if the outer surface of the monolayer has a tendency to bend inwards, towards the membrane interior. Furthermore, we use a Gaussian approximation, *i.e.*, we expand the free energy up to second order of z_i about a fully planar reference state. The total elastic energy of the coupled monolayer system is then given by [53,54,55,56]

$$\begin{aligned}\mathcal{F}_{\rm el} = \int \mathrm{d}^2 r \, \Big\{ & \frac{k_A}{8 t_0^2}(z_1 - z_2)^2 + \frac{k_c}{4}\big[(\Delta z_1)^2 + (\Delta z_2)^2\big] \\ & + k_c \frac{\zeta}{2 t_0}(z_1 - z_2)\big[\Delta z_1 - \Delta z_2\big] \\ & + k_c\big[c_1 \Delta z_1 - c_2 \Delta z_2\big] + \frac{\Gamma}{2}\big[\frac{1}{2}\nabla(z_1 + z_2)\big]^2 \Big\}\end{aligned} \quad (1)$$

Here we have not included the contribution of the Gaussian curvature, which is a constant for planar membranes with fixed topology [57]. The parameter t_0 is the mean monolayer thickness, k_A and k_c are the (bilayer) compression and bending modulus, respectively, ζ is a curvature-related parameter [53,54,55], and Γ the tension of the membrane [56].

We must briefly comment on the interpretation of the parameter Γ. It has been noted [58] and confirmed by simulations [59,60,61] that the externally applied tension (the "frame tension") and the tension experienced by the lipids inside the membrane (the "intrinsic" tension) differ slightly from each other in fluctuating membranes. However, fundamental symmetry considerations [62,63] suggest that the "tension" parameter governing the amplitude of membrane undulations coincides with the frame tension in the thermodynamic limit, except for a small multiplicative correction factor that accounts for the difference between the actual area and the area projected on the (x, y)-plane [64]. This implies that in a mean-field theory based on a quadratic approximation such as (1), the parameter Γ is most appropriately interpreted as a frame tension. Several simulations have confirmed that frame tension and fluctuation tension are equal [60,63,65,66,67], but deviations have also been reported, especially for low tensions [59,68,69,70]. If the membrane tension is close to zero, the existence of the thermodynamic limit for which the theoretical arguments [62,63] would apply becomes questionable. One consequence is that the amplitude of undulations may depend on the statistical ensemble under consideration [60]. However, these effects are small and we can neglect them in the context of this work. Hence we identify Γ with a frame tension, which can be applied and controlled externally.

We will also neglect the fact that the material parameters of the membrane may change under tension [56,71,72]. Our elastic model does not explicitly account for the effect of lipid orientation and possible lipid tilt [73,74,75,76,77]. A detailed consideration of such factors might help to establish a molecular basis for the relation between the elastic parameters and the lipid structure [78,79]. Here we wish to keep our model as simple as possible. We emphasize that Eq. (1) contains *all* terms up to second order of z_i and the spatial derivatives that are allowed by symmetry in a system of two coupled identical monolayers described by two surfaces z_i [80] (apart from the contribution of the Gaussian curvature). We have used the elastic model, Eq. (1), to fit deformation profiles in the vicinity of inclusions, with good results down to molecular length scales [55,81].

To describe lateral phase separation and domain formation within the monolayers, we supply each monolayer with an additional order parameter field $\varphi_i(x, y)$. Here φ is a collective variable designed to characterize the local lipid composition in a multicomponent system – not necessarily a binary system – with a propensity to locally phase separate. The associated free energy is described by a Ginzburg-Landau functional

$$\mathcal{F}_{\rm GL} = \int \mathrm{d}^2 r \Big\{ \sum_{i=1}^{2} \big[\frac{g}{2}(\nabla\varphi_i)^2 + \frac{t}{4}\varphi_i^2 + \frac{v}{8}\varphi_i^4\big] - \frac{s}{2}\varphi_1\varphi_2 \Big\} \quad (2)$$

with $v > 0$. The last term couples the compositions on the two leaflets and is constructed such that it favors equal composition for $s > 0$ (positive coupling) and different composition for $s < 0$ (negative coupling). In the absence of any coupling, lateral phase separation occurs for $t < 0$ and the monolayers remain homogeneous ($\varphi_i \equiv 0$) for $t > 0$. Hence the parameter t is temperature-like and describes the distance from the critical demixing transition in parameter space.

Thus far, we have combined standard theories for fluid elastic sheets and phase separating order parameter fields. The key additional feature that we must introduce to describe curvature-induced domain formation is a coupling between the order parameters $\varphi_i(x, y)$ and the local spontaneous curvature of the monolayer $c_i(x, y)$. Kollmitzer *et al.* [79] recently discussed how the monolayer curvature might depend on the membrane composition for raft-forming lipids. Specifically,

we assume that the relation between c_i and φ_i is roughly linear,

$$c_i(x,y) = c_0 + \hat{c}\,\varphi_i(x,y), \tag{3}$$

where c_0 is the spontaneous curvature in the mixed homogeneous system.

Eqs. (1) - (3) define our theoretical model. To proceed, we express the degrees of freedom in terms of a set of new fields that make the symmetries in the system more transparent: The position of the membrane midplane, $h(x,y) = \frac{1}{2}(z_1 + z_2)$, the variations of the local mean monolayer thickness, $u(x,y) = \frac{1}{2}(z_1 - z_2) - t_0$, the mean local order parameter $\Phi = \frac{1}{2}(\varphi_1 + \varphi_2)$, and the local order parameter difference between monolayer leaflets $\Psi = \frac{1}{2}(\varphi_1 - \varphi_2)$. Rewritten as a functional of these new fields, the total free energy reads

$$\begin{aligned}\mathcal{F} = \int \mathrm{d}^2 r \,\Big\{ & \frac{k_A}{2t_0^2}u^2 + \frac{k_c}{2}(\Delta u)^2 + 2k_c\frac{\zeta}{t_0}u\Delta u \\ & + \frac{\Gamma}{2}(\nabla h)^2 + \frac{k_c}{2}(\Delta h)^2 \\ & + \frac{g}{2}(\nabla\Phi)^2 + \frac{1}{2}(t-s)\Phi^2 + \frac{v}{4}\Phi^4 \\ & + \frac{g}{2}(\nabla\Psi)^2 + \frac{1}{2}(t+s)\Psi^2 + \frac{v}{4}\Psi^4 \\ & + 2k_c\hat{c}\,[\Phi\Delta u + \Psi\Delta h] + \frac{3}{2}v\,\Phi^2\Psi^2\Big\}.\end{aligned} \tag{4}$$

.

In this representation, it becomes clear that the two sets of fields (u,Φ) and (h,Ψ) are largely independent of each other. The only coupling between them is introduced by the last term in Eq. (4), a nonlinear fourth order term. The domain forming mechanism I is associated with modulations in the fields (h,Ψ) and mechanism II is associated with modulations in (u,Φ) (see Fig. 1).

Since the free energy (4) is quadratic in h and u, these degrees of freedom can be integrated out. Alternatively, we may adopt a mean-field approximation from the outset and minimize the free energy, Eq. (4), with respect to h and u. Apart from uninteresting constants, the result is the same and best written in a mixed Fourier- and real space representation (omitting constants):

$$\begin{aligned}\mathcal{F} = \frac{(2\pi)^2}{A}\sum_{\mathbf{q}}\Big\{ & \frac{1}{2}K_\Phi\big((\xi_0 q)^2\big)|\Phi_{\mathbf{q}}|^2 \\ & + \frac{1}{2}K_\Psi\big((\xi_\Gamma q)^2\big)|\Psi_{\mathbf{q}}|^2\Big\} \\ + \frac{v}{4}\int \mathrm{d}^2 r\,\Big\{ & \big(\Phi^4 + \Psi^4\big) + 6\,\Phi^2\Psi^2\Big\}\end{aligned} \tag{5}$$

with

$$K_\Phi(x) = t - s + \frac{g}{\xi_0^2}x - 4k_c\hat{c}^2\frac{x^2}{(1-x)^2 + \Lambda x} \tag{6}$$

$$K_\Psi(x) = t + s + \frac{g}{\xi_\Gamma^2}x - 4k_c\hat{c}^2\frac{x}{1+x}. \tag{7}$$

Here we have introduced the characteristic length scales $\xi_0 = (t_0^2 k_c/k_A)^{1/4}$ and $\xi_\Gamma = (k_c/\Gamma)^{1/2}$ and the dimensionless parameter $\Lambda = 2{-}4\zeta\sqrt{k_c/k_A}$. The length scale ξ_0 and the parameter Λ are intrinsic properties of the membrane. Experimentally, one finds that the bending rigidity, k_c, is roughly proportional to $k_A t_0^2$, hence ξ_0 should be of the order of the membrane thickness, $2t_0$. The parameter Λ characterizes the bilayer thickness profiles in the vicinity of a local perturbation [53, 55]: For $\Lambda \geq 4$, they decay towards the equilibrium thickness in a purely exponential manner; for $\Lambda < 4$, an oscillatory component emerges, and the membrane becomes unstable towards deformations at $\Lambda < 0$. Inserting numbers from experiments [82], all-atom simulations [54,83,84], or coarse-grained simulations [55] for the fluid phase of DPPC bilayers (dipalmitoyl phosphatidylcholine, of one of the most common lipids in natural biomembranes), one consistently obtains values around $\xi_0 \sim (0.9 - 1.4)$ nm, and $\Lambda \sim 0.7$ [49]. With typical experimental values for the tension [85,86] in the range of $\Gamma \sim 10^{-5}$N/m, one finds that ξ_Γ is of the order ~ 100 nm. It diverges for tensionless membranes.

- The parameter Λ, which characterizes the membrane material. It must be positive, otherwise the membrane is not stable
- The rescaled curvature coupling $\tilde{C} = 2\hat{c}\,\xi_0\sqrt{k_c/g}$
- The rescaled composition coupling $\tilde{s} = s\,\xi_0^2/g$
- The rescaled temperature parameter $\tilde{t} = t\,\xi_0^2/g$
- The rescaled tension $\tilde{\Gamma} = \Gamma\, t_0/\sqrt{k_c\, k_A}$

In this notation, the characteristic length scale ξ_Γ is simply given by $\xi_\Gamma = \xi_0/\sqrt{\tilde{\Gamma}}$.

Our task is to minimize the free energy (5) with respect to the fields Φ and Ψ, and to calculate the resulting phase diagrams. This is done in the next section.

3 Phase behavior of mixed bilayers

3.1 Stability analysis

At high "temperature" $\tilde{t}$, the system is disordered, $\Phi = \Psi \equiv 0$. The disordered state is unstable towards ordering or phase separation if either $K_\Phi(x)$ or $K_\Psi(x)$ become negative for at least one $x > 0$. Hence the instability limit is determined by the maximum value of t at which the minimum or K_Φ or K_Ψ becomes zero. Four types of instabilities are possible:

(i) Instability of $K_\Phi(x)$ at $x = 0$. This corresponds to an instability with respect to macroscopic demixing (state 2Φ in Fig. 1e)
(ii) Instability of $K_\Phi(x)$ at some $x > 0$. This corresponds to an instability with respect to a modulated state characterized by a periodic array of nanodomains (state nD in Fig. 1b)
(iii) Instability of $K_\Psi(x)$ at $x = 0$. This corresponds to an instability with respect to the formation of a globally asymmetric membrane (state ASY in Fig. 1d)
(iv) Instability of $K_\Psi(x)$ at some $x > 0$. This corresponds to an instability with respect to a modulated phase with a periodic array of microdomains (state μD in Fig. 1a)

The instabilities of K_Ψ ((iii) and (iv)) have been discussed by Shlomovitz and Schick [46]. At low curvature coupling $\tilde{C}$, the instability (iii) dominates and the membrane becomes asymmetric at $\tilde{t} = -\tilde{s}$. At high $\tilde{C}$, the instability (iv) takes over, and modulated microdomains with a wavelength $\lambda_\Psi = 2\pi\xi_0\tilde{\Gamma}^{-1/4}(\tilde{C} - \sqrt{\tilde{\Gamma}})^{-1/2}$ emerge for

$$\tilde{t} < \tilde{t}_\Psi := -\tilde{s} + (\tilde{C} - \sqrt{\tilde{\Gamma}})^2. \tag{8}$$

The two regimes are separated by a Lifshitz critical point at $\tilde{C} = \sqrt{\tilde{\Gamma}}$, at which point the wavelength λ_Ψ of the modulations diverges.

The picture that one obtains after analyzing the instabilities of K_Φ ((i) and (ii)) is similar, but the resulting scenario differs from that described above in one important aspect. At low curvature coupling $\tilde{C}$, the instability (i) dominates and the membrane phase separates at $\tilde{t} = \tilde{s}$. At high $\tilde{C}$, the instability (ii) dominates, and a modulated nanodomain phase emerges. However, the wavelength of this phase remains finite. The two regimes are connected by a bicritical point at $\tilde{C} = \sqrt{\Lambda}$ connecting a line of Ising-type transitions (regime (i)) and Brazovskii-type transitions [87] (regime (ii)), and the wavelength of the modulated phase at this point is $\lambda_\Phi = 2\pi\xi_0$. The transition point $\tilde{t}_\Phi$ between the modulated and the disordered phase at $\tilde{C} > \sqrt{\Lambda}$ is defined through a set of implicit equations

$$\epsilon := \frac{\tilde{C}^2}{\Lambda} - 1 = \frac{\delta^4 + 2\delta(1+\delta)^2\Lambda}{\Lambda(1+\delta)(\Lambda(1+\delta) - 2\delta)} \tag{9}$$

$$\tilde{t}_\Phi = \tilde{s} + \frac{\delta(1+\delta)(2+\delta)}{\Lambda(1+\delta) - 2\delta}, \tag{10}$$

where δ is related to the characteristic wavelength λ_Φ at the transition *via* $\lambda_\Phi = 2\pi\xi_0/\sqrt{1+\delta}$ and vanishes at the bicritical point. Close to the bicritical point, we can expand both equations in powers of δ, which leads to the expansion

$$\tilde{t}_\Phi - \tilde{s} = \epsilon\big[1 + \frac{\Lambda}{4}(\epsilon - \epsilon^2) + \frac{\Lambda}{16}(\Lambda + 4)\epsilon^3 + \mathcal{O}(\epsilon^4)\big]. \tag{11}$$

Far from the bicritical point, for large ϵ, one obtains the asymptotic behavior

$$\tilde{t}_\Phi - \tilde{s} \to \epsilon \begin{cases} 1 + \Lambda/(4-\Lambda) & \text{for } \Lambda < 2 \\ \Lambda & \text{for } \Lambda > 2. \end{cases} \tag{12}$$

Hence $\tilde{t}_\Phi - \tilde{s}$ is roughly proportional to ϵ in the whole range of $\tilde{C}$. Below, we will use the approximate expression derived from the leading order of the series expansion,

$$\tilde{t}_\Phi \approx \tilde{s} + \epsilon = \tilde{s} + \frac{1}{\Lambda}(\tilde{C}^2 - \Lambda). \tag{13}$$

In the total system of coupled order parameters, both the instabilities in Φ and Ψ can destroy the homogeneous membrane, and the membrane enters the phase associated with the instability at highest "temperature" $\tilde{t}$. Within the ordered or metastable phase, the nonlinear terms in the free energy expression, Eq. (5), become important, and we must include them to calculate the full phase diagram. This is done in the next section.

3.2 Phase diagrams

In the present work, we are not interested in the exact numerical solution of the free energy model, (4), but rather in a qualitative picture of the interplay of the different ordering mechanisms in the membrane. Therefore, we calculate the mean-field phase diagram within a single mode approximation which provides us with analytical expressions for the phase boundaries. Specifically, we make the following Ansatz for the shape of the order parameter field:

$$\Phi(\mathbf{r}) = \overline{\Phi}_m \cos(k_\Phi z) + \overline{\Phi}_s, \quad \Psi(\mathbf{r}) = \overline{\Psi}_m \cos(k_\Psi z) + \overline{\Psi}_s, \tag{14}$$

where $k_\Phi = 2\pi/\lambda_\Phi$ and $k_\Psi = 2\pi/\lambda_\Psi$ are the most unstable wavevectors for given $\tilde{C}$ and $\tilde{\Gamma}$ calculated in Sec. 3.1. Inserting this Ansatz in the functional (5), we obtain the free energy per area

$$\begin{aligned} F/A = \frac{v}{4}\Big\{ & \overline{\Phi}_m^2(\tilde{t} - \tilde{t}_\Phi) + 2\overline{\Phi}_s^2(\tilde{t} - \tilde{s}) \\ & + \overline{\Psi}_m^2(\tilde{t} - \tilde{t}_\Psi) + 2\overline{\Psi}_s^2(\tilde{t} + \tilde{s}) \\ & + \frac{3}{8}(\overline{\Phi}_m^4 + \overline{\Psi}_m^4) + \overline{\Phi}_s^4 + \overline{\Psi}_s^4 + 3(\overline{\Phi}_m^2\overline{\Phi}_s^2 + \overline{\Psi}_m^2\overline{\Psi}_s^2) \\ & + \frac{3}{2}\overline{\Phi}_m^2\overline{\Psi}_m^2 + 3(\overline{\Phi}_m^2\overline{\Psi}_s^2 + \overline{\Phi}_s^2\overline{\Psi}_m^2) + 6\overline{\Phi}_s^2\overline{\Psi}_s^2)\Big\}, \end{aligned} \tag{15}$$

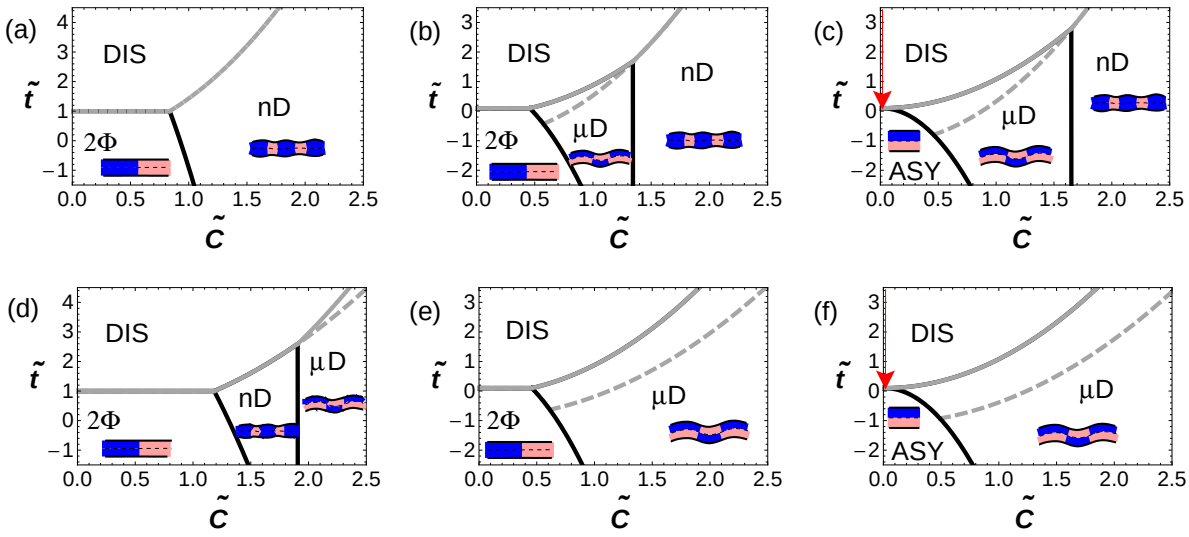

Fig. 2 Typical phase diagrams in the plane of "temperature" $\tilde{t}$ and curvature coupling $\tilde{C}$ for strong, weak, and negative monolayer composition coupling ($\tilde{s} = 1, 0.1, -0.1$) and two choices of the membrane parameter Λ, one with $\Lambda < 1$ and one with $\Lambda > 1$: (a) $\tilde{s} = 1, \Lambda = 0.7$; (b) $\tilde{s} = 0.1, \Lambda = 0.7$; (c) $\tilde{s} = -0.1, \Lambda = 0.7$; (d) $\tilde{s} = 1, \Lambda = 1.4$; (e) $\tilde{s} = 0.1, \Lambda = 1.4$; (f) $\tilde{s} = -0.1, \Lambda = 1.4$. The dimensionless tension is $\tilde{\Gamma} = 10^{-4}$ in all cases, corresponding to a characteristic length scale for microdomains of $\xi_\Gamma = 100\xi_0$. The membrane structures in the different phases correspond to those shown in Fig. 1. Solid gray lines correspond to continuous transitions, black lines to first order transitions, and dashed grey lines transition regions between a a pure μD phase (at high $\tilde{t}$) and a decorated μD phase which also contains nanodomains at the microdomain boundaries (at lower $\tilde{t}$). The red arrow indicates the position of a Lifshitz point.

which we can now minimize with respect to the amplitudes $\overline{\Phi}_m, \overline{\Phi}_s, \overline{\Psi}_m, \overline{\Psi}_s$ in a straightforward manner. We find that states with minimal free energy can only sustain one type of order, *i.e.*, all amplitudes are zero except, possibly, one. Transitions between different states are first order.

These predictions are consistent with the known behavior near Lifshitz critical points and seem reasonable in many other aspects as well. However, they clearly do not capture the interplay of microdomains and nanodomains in the limit $\xi_\Gamma/\xi_0 \to 0$ or $\tilde{\Gamma} \ll 1$ when the characteristic lengths of microdomains and nanodomains are very different. If the order parameter $\Psi(\mathbf{r})$ varies very slowly compared to $\Phi(\mathbf{r})$, it acts almost like a constant field on Φ, and it is clear that nanodomains might emerge in regions with $\Psi \approx 0$ even if the global amplitude of Ψ modulations does not vanish. Hence an adiabatic approximation seems more appropriate for this case, where $\overline{\Phi}_m$ is allowed to vary in space and to depend on the local value of Ψ^2.

Let us first assume that we can impose a given constant asymmetry Ψ on a mixed membrane with $\Phi \equiv 0$. As long as $\Psi^2 < \frac{1}{3}(\tilde{t}_\Phi - \tilde{t})$, the free energy (15) can then be lowered by introducing a periodic modulation with squared amplitude $\overline{\Phi}_m^2 = -\frac{4}{3}(\tilde{t} - \tilde{t}_\Phi + 3\Psi^2)$. The associated free energy gain per area is $F_m/A = -\frac{3v}{32}\overline{\Phi}_m^4$. If we now consider a modulated microdomain phase μD with very slowly varying order parameter $\Psi(\mathbf{r})$, we can lower the free energy by allowing for the formation of nanodomains at the interfaces between microdomains, and the associated adiabatic free energy can be approximated as

$$F_{\rm ad}/A = -\frac{v}{6}\int \mathrm{d}^2 r \left[\min\left(\tilde{t} - \tilde{t}_\Phi + 3\Psi(\mathbf{r})^2, 0\right)\right]^2. \quad (16)$$

However, the membrane is not entirely filled with nanodomains in this state, the nanodomains only build up in narrow regions close to the microdomain boundaries. The transition between the decorated μD and the nD phase remains discontinuous.

Combining all these results, we can now finally calculate the phase behavior of the coupled membrane system. Some representative phase diagrams for membranes with low tension are shown in Fig. 2. They feature the disordered phase at high "temperatures" $\tilde{t}$ and a variety of ordered and modulated states at low $\tilde{t}$. At low curvature coupling $\tilde{C}$, the low-temperature state is a homogeneous membrane, which is either phase separated (2Φ) for positive composition coupling $\tilde{s}$ across leaflets (Fig. 2a,b,d,e), or asymmetric (ASY) for negative coupling $\tilde{s}$ (Fig. 2c,f). At high curvature coupling $\tilde{C}$, both the modulated microdomain phase μD and the nanodomain phase nD may appear. Not surprisingly, the nanodomain phase tends to be favored if the composition coupling $\tilde{s}$ between leaflets is strongly positive (Fig. 2a,d). Another, less obvious factor that selects between modulated phases is the value of the membrane parameter Λ. This can be related to the different

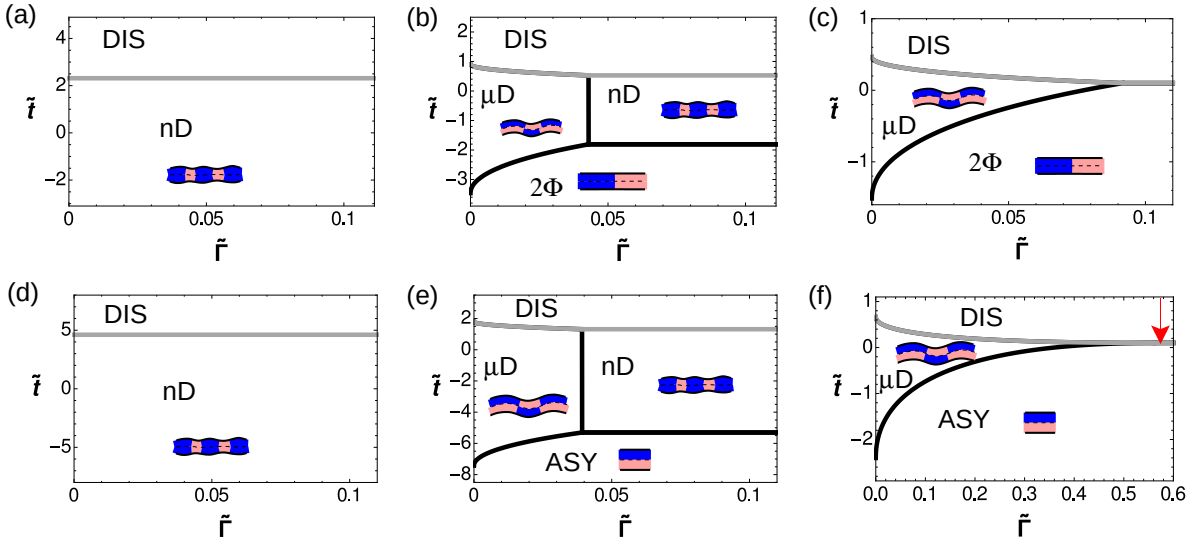

Fig. 3 Typical phase diagrams in the plane of "temperature" $\tilde{t}$ and dimensionless tension $\tilde{\Gamma}$ for $\Lambda = 0.7$ and different choices of monolayer composition coupling $\tilde{s}$ curvature coupling $\tilde{C}$. (a) $\tilde{s} = 0.1, \tilde{C} = 1.5$; (b) $\tilde{s} = 0.1, \tilde{C} = 1.$; (c) $\tilde{s} = 0.1, \tilde{C} = 0.75$; (d) $\tilde{s} = -0.1, \tilde{C} = 2.$; (e) $\tilde{s} = -0.1, \tilde{C} = 1.3$; (f) $\tilde{s} = -0.1, \tilde{C} = 0.75$; Solid gray lines correspond to continuous transitions, black lines to first order transitions, and red arrow indicates the position of a Lifshitz point.

slopes of $\tilde{t}_\Phi(\tilde{C})$ and $\tilde{t}_\Psi(\tilde{C})$. For small tensions, $\tilde{\Gamma} \ll 1$, and close to the bicritical point of Φ at $\tilde{C} = \sqrt{\tilde{\Gamma}}$, the slopes are given by $\mathrm{d}\tilde{t}_\Phi/\mathrm{d}\tilde{C} = 2\tilde{C}/\tilde{\Gamma}$ and $\mathrm{d}\tilde{t}_\Psi/\mathrm{d}\tilde{C} \approx 2\tilde{C}$. Hence the nanodomain state can supersede a microdomain state as $\tilde{C}$ increases if $\Lambda < 1$ (Fig. 2a-c), the microdomain state will remain dominant for $\Lambda > 1$ (Fig. 2d-f). We recall that phospholipid bilayers have values of Λ around 0.7. If this finding is representative for lipid bilayers, nanodomains would tend to be favored over microdomains at large curvature mismatch.

Fig. 2b-f) also indicates regions (in the μD phase below the dashed line), where we believe that nanodomains may exist within microdomains, based on the adiabatic approximation described above. Such states should be particularly interesting since they are filled with lines of nanodomains, either regularly ordered or – in case fluctuations destroy the global order – in a foam-like structure.

Next we study the influence of tension on the phase behavior. The results for selected parameter sets are shown in Fig. 3. As a rule, applying tension destabilizes the microdomain phase. This is also reported in Ref. [46]. With increasing tension, the temperature range where the microdomain phase is stable decreases and it is eventually replaced by the disordered structure, a nanodomain state, or a homogeneous membrane structure. The phase transitions between the other states are not affected by membrane tension.

We should note, however, that the tensions needed to bring about a phase transition are rather extreme. The tension unit used to rescale the dimensionless tension parameter $\tilde{\Gamma}$ is $\Gamma/\tilde{\Gamma} = \sqrt{k_c k_A}/t_0$, which corresponds to (50-100) mN/m for typical experimental values of the elastic parameters k_c and k_A/t_0^2 of phospholipid bilayers[82]. The tension strength where lipid bilayers rupture is typically around 2-10 mN/m [88]. On short time scales, higher tensions up to 20-30 mN/m can be sustained [89]. Still, the membranes will rupture for most of the tensions considered in Fig. 3. Also, it should be noted that membranes undergo significant structural rearrangement under high tension [56], which will likely interfere with domain formation. Hence, the phase diagrams shown in Fig. 3 are of rather academic interest with probably little practical relevance. The main control that one can exert by applying tension, according to our model, is to modulate the characteristic length scale of the microdomains. This could again be interesting in the mixed microdomain / nanodomain state, because it implies that tension can be used to manipulate the structural arrangements of microdomains.

4 Summary and discussion

In sum, we have presented a theoretical framework that allows us to describe two curvature-driven mechanisms for the formation of modulated structures in multicomponent lipid bilayers in a unified manner: A microdomain structure associated with a staggered composition profile on the two monolayers, and a nanodomain structure associated with domains that oppose each other on both monolayers. We have seen that both microdomain and nanodomain structures can be ob-

served for both negative and positive couplings between the lipid compositions on opposing monolayer leaflets. However, a strong positive coupling favors nanodomain formation and a strong negative coupling favors microdomain formation. We have also studied the influence of membrane tension and found, in agreement with Ref. [46], that microdomains are destabilized at high tensions. In our opinion, however, the most important effect of tension is that it can be used to control the characteristic wave length of the microdomains,

Our mean-field analysis revealed an unexpectedly complex phase behavior. It includes two types of Brazovskii-transitions and Ising transitions, bicritical points where Brazovskii lines meet with Ising lines or with each other, and possibly one Lifshitz point. We have considered the simplest possible system, a perfectly symmetric bilayer made of identical monolayers and a Ginzburg Landau free energy that is perfectly symmetric in the order parameter. These are the systems most often studied in laboratory experiments. The possible scenarios will be even more complicated if we consider asymmetric systems where, e.g., one order parameter is favored – which will create a competition between modulated phases with different symmetry [43] – or the lipid composition is different on both sides of the membranes [46]. Furthermore, we have assumed that only the spontaneous curvature is coupled to the local order parameter. In reality, one would expect all elastic parameters to depend on the local lipid composition [90]. In many cases, this will probably change the picture only in a quantitative sense, phase boundaries and length scales will be shifted. However, qualitatively new behavior may emerge if the Gaussian modulus becomes composition dependent. In that case, the contribution of the Gaussian curvature to the elastic free energy can no longer be neglected, and a new type of modulated phase may emerge that might be interesting in the context of membrane fusion.

In our mean-field approach, we have neglected fluctuations. They should have a severe impact on the phase diagrams. It is known that thermal fluctuations turn a continuous Brazovskii transition into a weak first order transition [87,91], and they destabilize Lifshitz points, such that a microemulsion channel may open up and/or part of the Ising critical line may become first order [47, 48]. Additionally, we have presented a simple scaling argument in Ref. [49] according to which nanodomain formation should preempt homogeneous demixing for *all* values of the curvature coupling $\tilde{C}$. The implications of this effect for the topology of the phase diagrams is still unclear. Most likely the Ising-type demixing transition at low $\tilde{C}$ will persist. As mentioned in the introduction, Ising-type demixing transitions have been observed in multicomponent membranes and the Ising critical exponents have been verified with great care [29,30,92]. However, the coexisting phases may be structured and contain a certain amount of nanodomains. The Brazovskii phases will become disordered in the vicinity of the mean-field Brazovskii line and be replaced by a relatively strongly structured microemulsion over a wide parameter range.

Thus the lateral structure of the membrane is presumably characterized by a combination of disordered micro- and nanodomains, where the nanodomains tend to accumulate along the borders of microdomains. Given their nanoscale size, the nanodomains can possibly be related to the lipid "rafts" discussed in the introduction. Our results indicate that microdomains can be used to manipulate rafts, but not vice versa. Since the size of the microdomains can be tuned by varying the applied tension, this reveals a way how the larger lateral organization of nanodomains or rafts could be controlled externally by a physical process.

According to the raft hypothesis, raft proteins use small lipid domains as templates, but they sometimes assemble to larger units to be functional [7]. We have seen how membrane tension could be used to assist such a process. However, our results rely on a mean-field theory and a number of further simplifying approximations. Studying the multicomponent system in detail by numerical simulations that also include thermal fluctuations will be the subject of future work.

Acknowledgements The ideas presented in this paper are based on previous work, mostly simulations, that were carried out by Stefan Dolezel, Gerhard Jung, Olaf Lenz, Sebastian Meinhardt, Jörg Neder, and Beate West. These simulations have given us trust in the coupled monolayer model which on which the present model is built. We also wish to thank Frank Brown, Laura Toppozini, Maikel Rheinstädter, and Richard Vink for collaborations that have helped to shape our view on lipid bilayers. We thank in particular Michael Schick for helpful comments on the manuscript and for pointing out Refs. [85,86,90].

References

1. Vereb, G., Szöllosi, J., Matko, J., Nagy, P., Farkas, T., Vigh, L., Matyus, L., Waldmann, T.A., Damjanovich, S.: Dynamic, yet structured: The cell membranes three decades after the singer-nicolson model. PNAS **100**, 8053–8058 (2003)
2. Singer, S.J., Nicolson, G.K.: Fluid Mosaic Model of Structure of Cell-Membranes. Science **175**(4023), 720–731 (1972)
3. Ahmed, S.N., Brown, D.A., London, E.: On the origin of sphingolipid/cholesterol-rich detergent-insoluble cell membranes: Physiological concentrations of cholesterol and sphingolipid induce formation of a detergent-

insoluble, liquid-ordered lipid phase in model membranes. Biochemistry **36**(36), 10,944–10,953 (1997)
4. Simons, K., Ikonen, E.: Functional rafts in cell membranes. Nature **387**, 569–572 (1997)
5. Brown, D.A., London, E.: Structure and origin of ordered lipid domains in biological membranes. J. Membr. Biology **164**(2), 103–114 (1998)
6. Pike, L.: Lipid rafts: Bringing order to chaos. J. Lip. Res. **44**, 655–667 (2003)
7. Pike, L.: Rafts defined: A report on the keystone symposium on lipid rafts and cell function. J. Lip. Res. **47**, 1597–1598 (2006)
8. Leslie, M.: Do lipid rafts exist? Science **334**, 1046–1047 (2011)
9. Lingwood, D., Simons, K.: Lipid rafts as a membrane-organizing principle. Science **327**, 46–50 (2010)
10. Eggeling, C., Ringemann, C., Medda, R., Schwarzmann, G., Sandhoff, K., Polyakova, S., Belov, V.N., Hein, B., von Middendorf, C., Schönle, A., Hell, S.W.: Direct observation of the nanoscale dynamics of membrane lipids in a living cell. Nature **457**, 1159–1162 (2009)
11. Mizuno, H., Abe, M., Dedecker, P., Makino, A., Rocha, S., Ohno-Iwashita, Y., Hofkens, J., Kobayashi, T., Miyawaki, A.: Fluorescent probes for superresolution imaging of lipid domains on the plasma membrane. Chemical Science **2**, 1548–1553 (2011)
12. Owen, D.M., Magenau, A., Williamson, D., Gaus, K.: The lipid raft hypothesis revisited – new insights on raft composition and function from super-resolution fluorescence microscopy. Bioessays **34**, 739–747 (2012)
13. Koynova, R., Caffrey, M.: Phases and phase transitions of the phosphatidylcholines. Biochimica et Biophysica Acta - Reviews on Biomembranes **1376**, 91–145 (1998)
14. Koynova, R., Caffrey, M.: An index of lipid phase diagrams. Chemistry and Physics of Lipids **115**, 107–219 (2002)
15. Katsaras, J., Tristram-Nagle, S., Liu, Y., Headrick, R.L., Fontes, E., Mason, P.C., Nagle, J.F.: Clarification of the ripple phase of lecithin bilayers using fully hydrated, aligned samples. Phys. Rev. E **61**, 5668–5677 (2000)
16. Leidy, C., Kaasgaard, T., Crowe, J.H., Mouritsen, O.G., Jorgensen, K.: Ripples and the formation of anisotropic lipid domains: imaging two-component supported double bilayers by atomic force microscopy. Biophys. J. **83**, 2625–2633 (2002)
17. Lenz, O., Schmid, F.: Structure of symmetric and asymmetric ripple phases in lipid bilayers. Phys. Rev. Lett. **98**, 058,104 (2007)
18. Schmid, F., Dolezel, S., Loenz, O., Meinhard, S.: On ripples and rafts: Curvature induced nanoscale structures in lipid membranes. J. Phys.: Conf. Series **487**, 012,004 (2014)
19. Connell, S.D., Heath, G., Olmsted, P.D., Kisil, A.: Critical point fluctuations in supported lipid membranes. Faraday Disc. **161**, 91–111 (2013)
20. Armstrong, C.L., Marquardt, D., Dies, H., Kucerka, N., Yamani, Z., Harroun, T.A., Katsaras, J., Shi, A.C., Rheinstädter, M.C.: The observation of highly ordered domains in membranes with cholesterol. PLoS One **8**, E66,162 (2013)
21. Rheinstädter, M.C., Mouritsen, O.G.: Small-scale structure in fluid cholesterol-lipid bilayers. Current Opinion in Colloid & Interface Science **18**, 440–447 (2013). DOI 10.1016/j.cocis.2013.07.001
22. Toppozini, L., Meinhardt, S., Armstrong, C.L., Yamani, Z., Kuvcerka, N., Schmid, F., Rheinstädter, M.: The structure of cholesterol in lipid rafts. Phys. Rev. Lett. **113**, 228,101 (2014)
23. Nickels, J.D., Cheng, X., Mostofian, B., Stanley, C., Lindner, B., Heberle, F.A., Perticaroli, S., Feygenson, M., Egami, T., Standaert, R.F., Smith, J.C., Myles, D.A.A., Ohl, M., Katsaras, J.: Mechanical properties of nanoscopic lipid domains. J. Am. Chem. Soc. p. just accepted (2015). DOI 10.1021/jacs.5b08894
24. Baumgart, T., Hess, S.T., Webb, W.W.: Imaging coexisting fluid domains in biomembrane models coupling curvature and line tension. Nature **425**, 821–824 (2003)
25. Veatch, S.L., Keller, S.L.: Separation of liquid phases in giant vesicles of ternary mixtures of phospholipids and cholesterol. Biophys. J. **85**(5), 3074–3083 (2003)
26. Veatch, S.L., Keller, S.L.: Seeing spots: Complex phase behavior in simple membranes. Biochimica et Biophysica Acta **1746**, 172–185 (2005)
27. Veatch, S.L., Keller, S.L.: Miscibility phase diagrams of giant vesicles containing sphingomyelin. Phys. Rev. Lett. **94**, 148,101 (2005)
28. Veatch, S.L., Cicuta, P., Sengupta, P., Honerkamp-Smith, A.R., Holowka, D., Baird, B.: Critical fluctuations in plasma membrane vesicles. ACS Chem. Biol. **3**, 287–293 (2008)
29. Veatch, S.L., Soubias, O., Keller, S.L., Gawrisch, K.: Critical fluctuations in domain-forming lipid mixtures. PNAS **104**, 17,650–17,655 (2007)
30. Honerkamp-Smith, A.R., Cicuta, P., Collins, M.D., Veatch, S.L., den Nijs, M., Schick, M., Keller, S.J.: Line tensions, correlation lengths, and critical exponents in lipid membranes near critical points. Biophys. J. **95**, 236–246 (2008)
31. Honerkamp-Smith, A.R., Veatch, S.L., Keller, S.J.: An introduction to critical points for biophysicists: Observations of compositional heterogeneity in lipid membranes. Biochimica et Biophysica Acta **1788**, 53–63 (2009)
32. Komura, S., Andelman, D.: Physical aspects of heterogeneities in multi-component lipid membranes. Adv. Coll. Interf. Sci. **208**, 34–46 (2014)
33. Simons, K., Vaz, W.L.C.: Model systems, lipid rafts, and cell membranes. Annu. Rev. Biophys. Biomol. Struct. **33**, 269–295 (2004)
34. Brewster, R., Pincus P. A. Safran, S.A.: Hybrid lipids as a biological surface-active component. Biophys. J. **97**, 1087–1094 (2009)
35. Hirose, Y., Komura, S., Andelman, D.: Coupled modulated bilayers: A phenomenological model. ChemPhysChem **10**, 2839–2846 (2009)
36. Yamamoto, T., Brewster, R., Safran, S.A.: Chain ordering of hybrid lipids can stabilize domains in saturated/hybrid/cholesterol lipid membranes. EPL **91**, 28,002 (2010)
37. Yamamoto, T., Safran, S.A.: Line tension between domains in multicomponent membranes is sensitive to the degree of unsaturation of hybrid lipids. Soft Matter **7**, 7021–7033 (2011)
38. Hirose, Y., Komura, S., Andelman, D.: Concentration fluctuations and phase transitions in coupled modulated bilayers. Phys. Rev. E **86**, 021,916 (2012)
39. Palmieri, B., Safran, S.A.: Hybrid lipids increase the probability of fluctuating nanodomains in mixed membranes. Langmuir **29**, 5246–5261 (2013)
40. Palmieri, B., Yamamoto, T., Brewster, R.C., Safran, S.A.: Line active molecules promote inhomogeneous structures in membranes: Theory, simulations and experiments. Adv. Coll. Interf. Sci. **208**, 58–65 (2014)
41. Leibler, S., Andelman, D.: Ordered and curved mesostructures in membranes and amphiphilic films. J. de Physique **48**, 2013–2018 (1987)

42. Safran, S.A., Pincus, P., Andelman, D.: Theory of spontaneous vesicle formation in surfactant mixtures. Science **248**, 354–356 (1990)
43. Kumar, P.B.S., Gompper, G., Lipowsky, R.: Modulated phases in multicomponent fluid membranes. Phys. Rev. E **60**, 4610–4618 (1999)
44. Harden, J.L., MacKintosh, F.C.: Shape transformations of domains in mixed-fluid films and bilayer membranes. Europh. Lett. **28**, 495–500 (1994)
45. Schick, M.: Membrane heterogeneity: Manifestation of a curvature-induced microemulsion. Phys. Rev. E **85**, 031,902 (2012)
46. Shlomovitz, R., Schick, M.: Model of a raft in both leaves of an asymmetric lipid bilayer. Biophys. J. **105**, 1400–1413 (2013)
47. Shlomovitz, R., Maibaum, L., Schick, M.: Macroscopic phase separation, modulated phases, and microemulsions: A unified picture of rafts. Biophys. J. **106**, 1979–1985 (2014)
48. Sadeghi, S., Müller, M., Vink, R.L.C.: Raft formation in lipid bilayers coupled to curvature. Biophys. J. **107**, 1591–1600 (2014)
49. Meinhardt, S., Vink, R.L.C., Schmid, F.: Monolayer curvature stabilizes nanoscale raft domains in mixed lipid bilayers. PNAS **12**, 4476–4481 (2013)
50. Collins, M.D., Keller, S.L.: Tuning lipid mixtures to induce or suppress domain formation across leaflets of unsupported asymmetric bilayers. PNAS **105**, 124–128 (2008)
51. Dan, N., Pincus, P., Safran, S.A.: Membrane-induced interactions between inclusions. Langmuir **9**, 2768–2771 (1993)
52. Dan, N., Berman, A., Pincus, P., Safran, S.A.: Membrane-induced interactions between inclusions. J. de Physique II **4**, 1713–1725 (1994)
53. Aranda-Espinoza, H., Berman, A., Dan, N., Pincus, P., Safran, S.: Interaction between inclusions embedded in membranes. Biophys. J. **71**, 648–656 (1996)
54. Brannigan, G., Brown, F.: A consistent model for thermal fluctuations and protein-induced deformations in lipid bilayer. Biophys. J. **90**, 1501–1520 (2006)
55. West, B., Brown, F.L.H., Schmid, F.: Membrane-protein interactions in a generic coarse-grained model for lipid bilayers. Biophys. J. **96**, 101–115 (2009)
56. Neder, J., West, B., Nielaba, P., Schmid, F.: Coarse-grained simulations of membranes under tension. J. Chem. Phys. **132**, 115,101 (2010)
57. Safran, S.A.: Statistical Thermodynamics of Surfaces, Interfaces, and Membranes. Perseus Books, Cambridge, Massachusetts (1994)
58. Farago, O., Pincus, P.: The effect of thermal fluctuations on schulman area elasticity. Eur. Phys. J. E **11**, 399–408 (2003)
59. Fournier, J.B., Barbetta, C.: Direct calculation from the stress tensor of the lateral surface tension of fluctuating fluid membranes. Phys. Rev. Lett. **100**, 078,103 (2008)
60. Schmid, F.: Are stress-free membranes really "tensionless"? EPL **95**, 28,008 (2011)
61. Shiba, H., Noguchi, H., Fournier, J.B.: Monte carlo study of the frame, fluctuation and internal tensions of fluctuating membranes with fixed area. arxiv:1507.08722 (2015)
62. Cai, W., Lubensky, T.C., Nelson, P., Powers., T.: Measure factors, tension, and correlations of fluid membranes. J. de Physique II **4**, 931–949 (1994)
63. Farago, O., Pincus, P.: Statistical mechanics of bilayer membrane with a fixed projected area. J. Chem. Phys. **120**, 2934–2950 (2004)
64. Diamant, H.: Model-free thermodynamics of fluid vesicles. Phys. Rev. E **84**, 0611,203 (2011)
65. Wang, Z.J., Frenkel, D.: Modeling flexible amphiphilic bilayers: A solvent-free off-lattice Monte Carlo study. J. Chem. Phys. **122**, 234,711 (2005)
66. Noguchi, H., Gompper, G.: Meshless membrane model based on the moving least-squares method. Phys. Rev. E **73**, 021,903 (2006)
67. Farago, O.: Mechanical surface tension governs membrane thermal fluctuations. Phys. Rev. E **84**, 051,944 (2011)
68. Imparato, A.: Surface tension in bilayer membranes with fixed projected area. J. Chem. Phys. **124**, 154,714 (2006)
69. Stecki, J.: Balance of forces in simulated bilayers. J. Phys. Chem. B **112**(14), 4246–4252 (2008)
70. Tarazona, P., Chacon, E., Bresme, F.: Thermal fluctuations and bending rigidity of bilayer membranes. J. Chem. Phys. **139**, 094,902 (2013)
71. Akimov, S.A., Kuzmin, P.I., Zimmerberg, J., Cohen, F.S.: Lateral tension increases the line tension between two domains in a lipid bilayer membrane. Phys. Rev. E **75**, 011,919 (2005)
72. Watson, M.C., Morriss-Andrews, A., Welch, P.M., Brown, F.L.H.: Thermal fluctuations in shape, thickness, and molecular orientation in lipid bilayers ii: Finite surface tensions. J. Chem. Phys. **139**, 084,706 (2013)
73. Fournier, J.B.: Coupling between membrane tilt-difference and dilation: A new "ripple" instability and multiple crystalline inclusions phases. Europh. Lett. **43**, 725–730 (1998)
74. Fournier, J.B.: Microscopic membrane elasticity and interactions among membrane inclusions: Interplay between the shape, dilation, tilt and tilt-difference modes. Eur. Phys. J. B **11**, 261–272 (1999)
75. Bohinc, K., Kralj-Iglic, V., May, S.: Interaction between two cylindrical inclusions in a symmetric lipid bilayer. J. Chem. Phys. **119**, 7435–7444 (2003)
76. Fošnarič, M., Iglič, A., May, S.: Influence of rigid inclusions on the bending elasticity of a lipid membrane. Phys. Rev. E **74**, 051,503 (2006)
77. Watson, M.C., Penev, E.S., Welch, P.M., Brown, F.L.H.: Thermal fluctuations in shape, thickness, and molecular orientation in lipid bilayers. J. Chem. Phys. **135**, 244,701 (2011)
78. Kuzmin, P.I., Akimov, S.A., Chizmadzhev, Y.A., Zimmerberg, J., Cohen, F.S.: Line tension and interaction energies of membrane rafts calculated from lipid splay and tilt. Biophys. J. **88**, 1120–1133 (2005)
79. Kollmitzer, B., Heftberger, P., Rappolt, M., Pabst, G.: Monolayer spontaneous curvature of raft-forming membrane lipids. Soft Matter **9**, 10,877–10,884 (2013)
80. Schmid, F.: Fluctuations in lipid bilayers: Are they understood? Biophysical Reviews and Letters **8**, 1–20 (2013). DOI 10.1142/S1793048012300113
81. Neder, J., Nielaba, P., West, B., Schmid, F.: Interactions of membranes with coarse-grain proteins: A comparison. New J. of Physics **14**, 125,017 (2012)
82. Marsh, D.: Elastic curvature constants of lipid monolayers and bilayers. Chemistry and Physics of Lipids **144**, 146–159 (2006)
83. Lindahl, E., Edholm, O.: Mesoscopic undulations and thickness fluctuations in lipid bilayers from molecular dynamics simulations. Biophys. J. **79**, 426–433 (2000)
84. Marrink, S.J., Risselada, H.J., Yefimov, S., Tielemann, D.P., de Vries, A.H.: The martini force field: Coarse grained model for biomolecular simulations. J. Phys. Chem. B **111**, 7812–7823 (2007)

85. Gauthier, N.C., Masters, T.A., Sheetz, M.: Mechanical feedback between membrane tension and dynamics. Trends Cell Biol. **22**, 527–535 (2012)
86. Pontes, B., Ayala, Y., Fonseca, A., Romao, L., Amaral, R., Salgado, L., Lima, F.R., Farina, M., Viana, N.B., Moura-NEto, V., Nussenzveig, H.M.: Membrane elastic properties and cell function. PLOS one **8**, 67,708 (2013)
87. Brazovskii, S.A.: Phase transitions of an isotropic system to a nonuniform state. Soviet Physics JETP **41**, 85–89 (1975)
88. Needham, D., Nunn, R.S.: Elastic deformation and failure of lipid bilayer membranes containing cholesterol. Biophys. J. **58**, 997–1009 (1990)
89. Evans, E., Heinrich, V., Ludwig, F., Rawicz, W.: Dynamic tension spectroscopy and strength of biomembranes. Biophys. J. **85**, 2342–2350 (2003)
90. Amazon, J.J., Goh, S.L., Feigenson, G.W.: Competition between line tension and curvature stabilizes modulated phase patterns on the surface of giant unilamellar vesicles: A simulation study. Phys. Rev. E **87**, 022,708 (2013)
91. Hohenberg, P.C., Swift, J.B.: Metastability in fluctuation-driven first-order transitions: Nucleation of lamellar phases. Phys. Rev. E **52**, 1828–1845 (1995)
92. Honerkamp-Smith, A.R., Machta, B.B., Keller, S.J.: Experimental observations of dynamic critical phenomena in a lipid membrane. Phys. Rev. Lett. **108**, 26,507 (2012)